The Zeiss-Nomarski differential interference equipment for transmitted-light microscopy

By R. D. Allen, G. B. David, G. Nomarski

With 19 figures

Reprinted from
Zeitschrift für wissenschaftliche Mikroskopie und mikroskopische Technik
Band 69, Heft 4 (1969)
S. Hirzel Verlag, Stuttgart

The Zeiss-Nomarski differential interference equipment for transmitted-light microscopy

By **R. D. Allen, G. B. David, G. Nomarski**

With 19 figures

Introduction

Equipment for differential interference contrast in transmitted light microscopy designed by NOMARSKI (1952, 1955) and manufactured under licence from the C.N.R.S. by Carl Zeiss/Oberkochen (German Federal Republic), has recently become generally available. It is one of a series of devices that rely on the interference of a pair of wavefronts (PILLER, 1962) to generate contrast, and it is constructed in such a way that it can be used as an accessory on the standard Zeiss microscopes. A brief description was issued by the manufacturers in December, 1968 (Zeiss-Publication). The Zeiss equipment necessary for differential interference microscopy in transmitted light comprises the following accessories: (I) a single beam-splitting slide, consisting of a modified quartz Wollaston prism oriented at 45° to an attached analyser, and mounted in a screw-driven carriage (so that a variable amount of bias compensation can be introduced at will), which is accommodated in the normal analyser slot between the objectives and eyepiece; (II) a strain-free achromatized condenser, fitted with three auxiliary modified Wollaston prisms, in addition to two annular stops for phase-contrast microscopy (Zeiss-Publication, 1968). A detailed theoretical and practical evaluation of the prototype was undertaken by us over the last four years, at the request of Dr. HORST PILLER of Carl Zeiss. The results were presented at the Centenary Conference of the Royal Microscopical Society in London, 1966 (ALLEN, DAVID, HIRSH, 1966; DAVID, ALLEN, HIRSH, WATTERS, 1966). These will be published in full later, in the Journal of the Royal Microscopical Society.

The purposes of the present paper are to illustrate and to describe briefly some of the properties of differential interference microscopes. This paper is complementary to, and should be read in conjunction with, the Zeiss description of the equipment now being produced (1966). It is meant as an introduction to differential interference microscopy for those who until now used only phase-contrast microscopy and image-duplication (PILLER, 1962) interference microscopy in their work, and as a short practical guide to the interpretation of differential interference images. Several hundred scientists have already acquired the Zeiss/Nomarski equipment in the brief period since our first publications about it (ALLEN et al., 1966; DAVID et al., 1966; BAJER, ALLEN, 1966; BAJER, ALLEN, 1966), and it is becoming an indispensable tool for biological and medical work of many kinds. The discussion that follows (except for

constructional details and a few factors relating to performance) is also applicable in a general way to alternative designs of differential interference microscopes (FRANÇON, 1953, 1961; FRANÇON, YAMAMOTO, 1962) produced by other manufacturers.

The principal advantages of the Zeiss/Nomarski design in biological work are: (I) Images of phase-objects are perceived as though "shadow-cast"; differential interference contrast is a function of the gradient in phase difference across the objects, and there is a related azimuth effect. These properties facilitate the interpretation of images of complicated objects. (II) Exceptionally high resolution and contrast are obtainable simultaneously for a wide range of objects, including many biological objects that do not produce useful images with other methods of optical microscopy. (III) Contrast can be varied instrumentally to suit the object. (IV) Because maximum contrast is obtained at a large aperture of the condenser, the high lateral resolution of the instrument is matched by a corresponding shallowness of the depth of field. This readily permits the "optical sectioning" of relatively thick biological objects, with exceptional freedom from spurious contrast due to out-of-focus object details, which is so often troublesome in phase-contrast systems. (V) Extended objects (e. g. organized tissue-cultures, whole animals and embryos, thick and even ultra-thin microtome sections) can be examined as well as separate objects, which is not the case with the image-duplication interference equipment. (VI) Amplitude and mixed phase-amplitude objects (e. g. stained sections, naturally pigmented protists and other cells, Feulgen-treated chromosome spreads) can be examined as readily as pure phase objects, and the optical properties of the differential interference instrument then enhance the contrast due to absorption.

The differential interference contrast equipment does not render image-duplication interference and phase-contrast microscopes obsolete. It is one more tool – a particularly valuable one – with which to probe the interaction between radiation and matter, a tool to be used systematically in conjunction with the other methods of microscopy (SWANN, MITCHISON, 1950). The image-duplication interference microscope remains the instrument of choice for quantitative refractometry of small objects, and the phase-contrast microscope for the morphological study of extended objects that are either too anisotropic or require too large a condenser working distance to be examined profitably under the existing differential interference microscopes.

How is the "shadow-cast" image formed?

Upon examining the image of a transparent microscopic object with the differential interference equipment for the first time, it is easy to be misled by the beautiful plasticity of the resulting pattern of highlights and shadows into supposing that the differential equipment yields true 3-dimensional images, and that the actual surface topography of an object can be perceived directly. This impression is totally erroneous for the majority of biological specimens. The sole exceptions are: backed replicas and simple interfaces between media of different refractive index. It is of the greatest practical importance to master the very simple physical principles which govern the generation of the "shadow-cast" effect. Only thus can errors of interpretation be avoided, and the microscope be properly adjusted for optimum results.

The Zeiss/Nomarski differential interference contrast equipment for transmitted light is simply a polarizing two-beam shearing interference device, in which the lateral separation between the two interfering beams is very small. The principle of operation of the differential interference microscope equipment is best understood by comparing it with the related and more familiar image-duplication equipment (PILLER, 1962).

Basic design

Both instruments can be considered to be modified polarizing microscopes, fitted with birefringent beam-splitters, auxiliary prisms and bias compensators (ALLEN et al., 1966; DAVID et al., 1966). The arrangement of the three instruments is illustrated in Fig. 1 (see also PILLER, 1962; Zeiss-Publication, 1968; ALLEN et al., 1966; DAVID

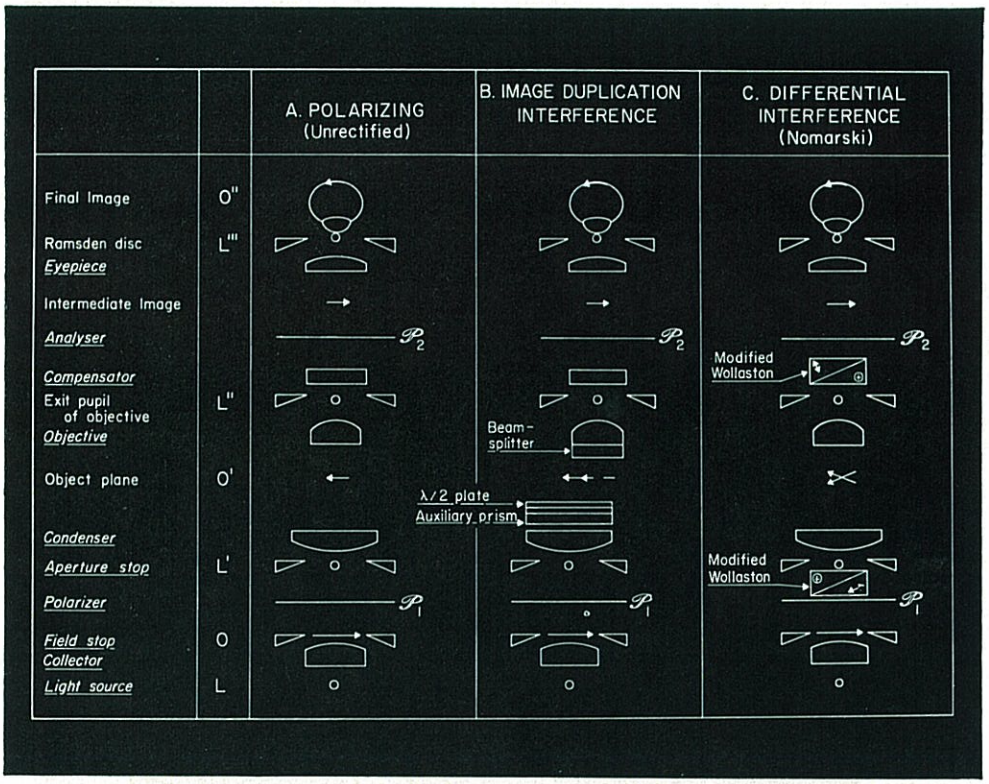

Fig. 1. Diagrammatic representation of the arrangement of the major optical components in the basic polarizing (A), and the derived image-duplication (B), and differential (C) interference microscopes. The interference microscopes differ from the parent instrument in that birefringent crystal accessories are used to split the incident beam into two mutually coherent components that are capable of interfering; in the image-duplication instrument, the beam-splitter is a calcite plate, and in the differential instrument, a modified Wollaston quartz prism. In both cases, the beam-splitter is matched by an auxiliary crystal component that cancels out the birefringence of the beam-splitter, therefore providing an even background. In this diagram, the axial location of pupillary planes is indicated by open circles, and of field planes by suitably oriented arrows.

et al., 1966). In both interference instruments, the optical object (defined as the plane wavefront that is retarded or advanced by the microscopic object) is sheared laterally by the beam-splitter in a direction at 45° to the plane of polarization of the incident beam (Northwest-Southeast as one looks down the eyepiece). The optical object is divided into two laterally separated wavefronts in the plane of the image; these wavefronts, being coherent, interfere after passing through the analyser, giving rise to interference contrast. Two separate image points are obtained for each point in the optical object. At any point in the beam emerging from the analyser, the intensity (I) is a function of the phase difference in radians ($\Delta(A')$), between the interfering wavefronts (Σ') at the point A':

$$I \cong I_{\max} \sin^2 \tfrac{1}{2} \Delta(A') + I_{\min} \tag{1}$$

where $I_{\max}$ is the maximum intensity transmitted by the system, $I_{\min}$ the minimum possible intensity (Zeiss-Publication, 1968; ALLEN et al., 1966; DAVID et al., 1966), and $\Delta(\Sigma')$ the phase difference between the interfering beams at that point.

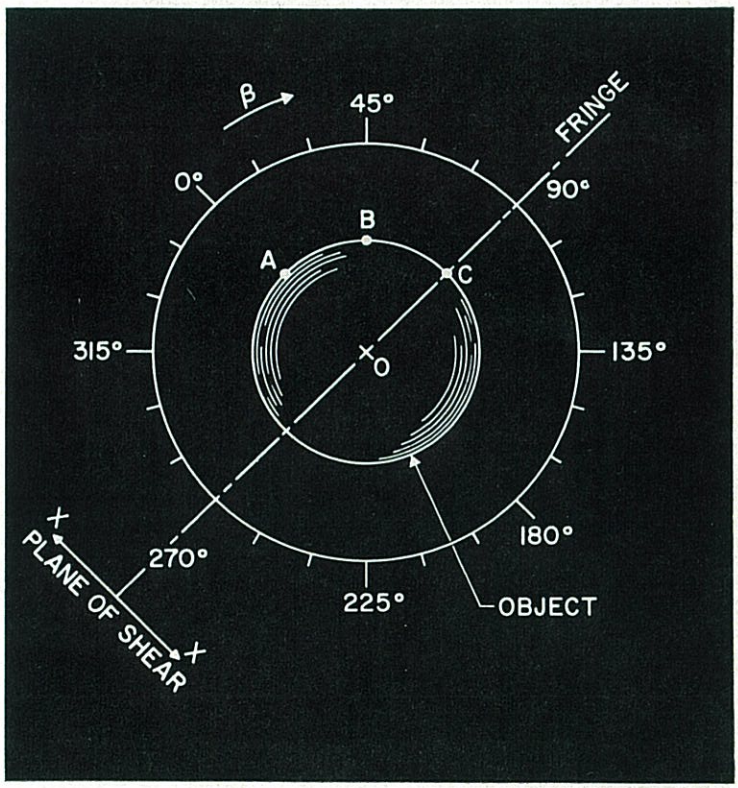

Fig. 2. Diagrammatic representation of a flattened spheroid (e. g. a nucleus) in the field of an interference microscope. $X-X$ represents the direction of shear of the beam-splitter (calcite plate in the image-duplication instrument, modified Wollaston in the differential). The azimuth angle β is measured from the direction of shear. Points A, B, and C, define three azimuths through the object. See text and Figs. 3–5.

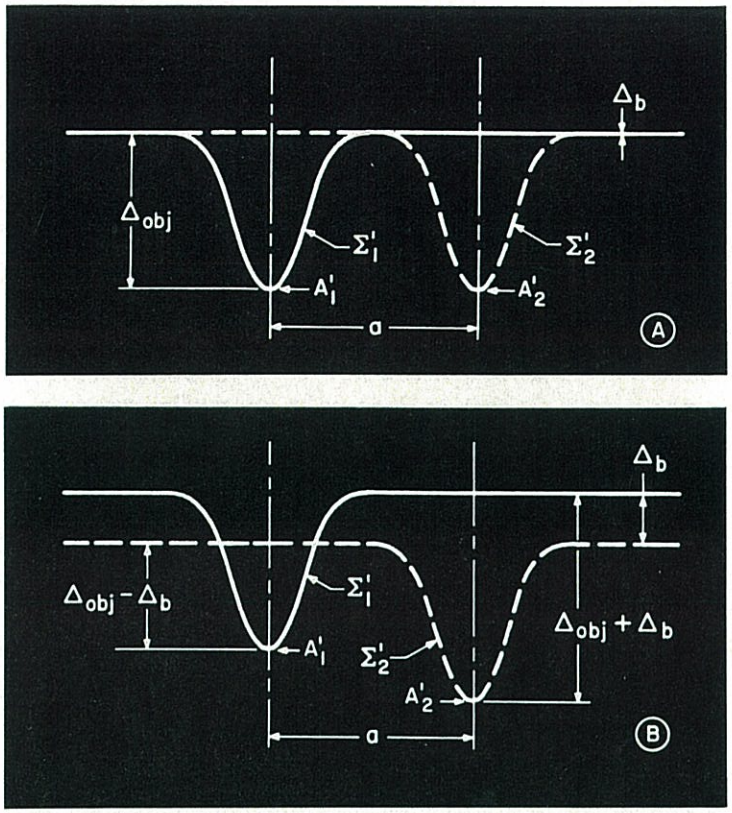

Fig. 3. Sheared wavefronts in the primary image plane of the image-duplication interference microscope obtained for the object drawn in Fig. 2. In (A) the microscope was set at extinction, and in (B) a positive bias retardation, Δ_b, was added. The wavefront is a representation of the profile or elevation of a plane wave, Σ, that we imagine moves along the optical axis of the microscope, is retarded or advanced in places as it interacts with the microscopic object (thereby becoming the "optical object", Σ), and is finally sheared by the beam-splitter into two wavefronts. The sheared wavefronts are represented in Fig. 3 by Σ'_1 and Σ'_2. The retardation introduced by the dephasing object is Δ_{obj}, and a is the distance of shear produced by the beam-splitter in the plane of the image. See text, and Figs. 2, 4—5.

The differences in the kinds of images obtained with the two instruments are attributable to the difference in the amount of shear produced by their beam-splitters. In the image-duplication system, the distances of shear in the plane of the object when using the objective-condenser sets 10/0.22, 40/0.65, and 100/1.0, are 560 μm, 180 μm, and 56 μm, respectively. In the differential system, the corresponding figures for the 16/0.32, 40/0.65, and 100/1.25 objectives, are approximately 1.32 μm, 0.55 μm, and 0.22 μm, respectively.

The consequences of small shear are more easily understood by considering an example. Let the microscopic object be a small flattened spheroid (say, the nucleus of a fibroblast of about 20 μm in diameter), phase-retarding in relation to its surround. This object is represented in Fig. 2. The corresponding sheared wavefronts

in the plane of the primary image are represented in Fig. 3 for the image-duplication equipment, and in Fig. 4 for the differential equipment. We shall consider 3 azimuths of the globule (Fig. 2): *AO*, *BO*, and *CO*, respectively parallel to, at 45°, and at right angles to the direction of shear, *XX*. We shall also consider the effects of varying bias compensation.

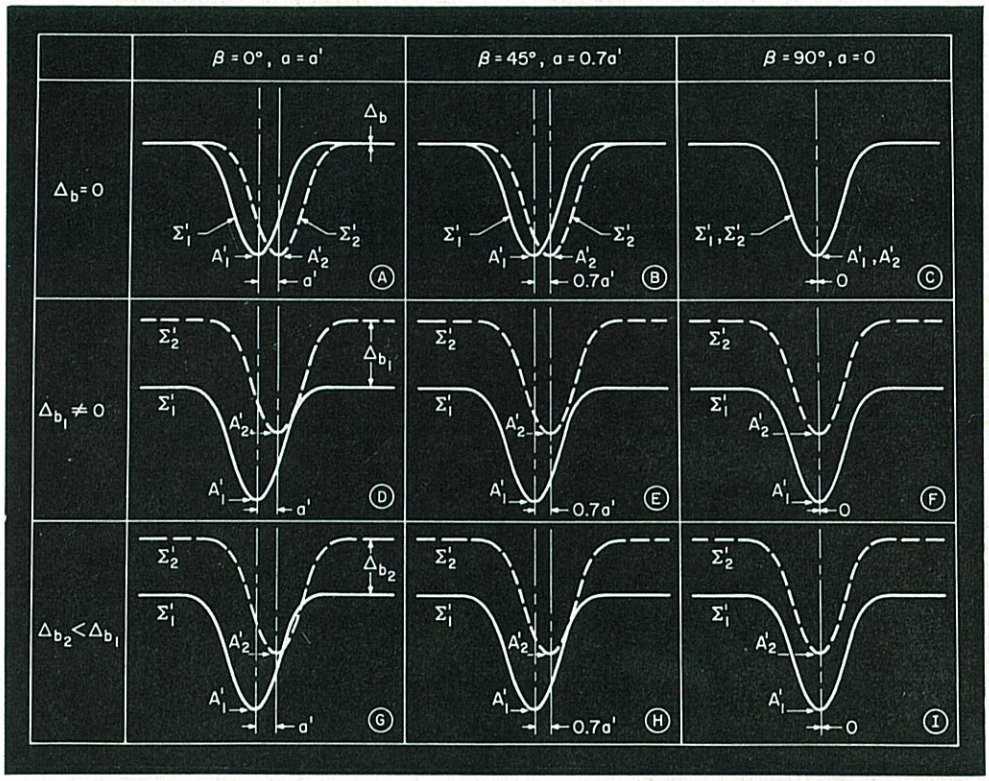

Fig. 4. Sheared wavefronts in the primary image plane of the differential interference microscope obtained for the object drawn in Fig. 2. To keep the diagram to reasonable dimensions, the object is now given a diameter of 2 μm. Nine combinations of azimuths and bias retardations are drawn. The diagram indicates how the effective lateral separation between the interfering wavefronts decreases as the azimuth increases between 0 and 90° (azimuths *AO*, *BO* and *CO* of Fig. 2), and how bias compensation can be used to achieve maximum contrast at various azimuths (*D* and *G*). See text and Figs. 2—3, 5.

Fig. 3 A represents the sheared wavefronts (Σ_1' and Σ_2') in the image-duplication interference equipment, when the bias compensator is adjusted to produce zero retardation between the wavefronts in the region of the background ($\Delta_b = 0$). The wavefronts are laterally sheared by a distance a (56 μm in the case of the oil-immersion objective), which is large in relation to the dimensions of the dephasing object (ca. 20 μm). There is now no lateral overlap at all between the wavefronts in the region of the object. Point A_1' lies directly under the plane portion of the "reference" sheared wavefront Σ_2', and point A_2' under a corresponding plane portion of wave-

front Σ_1'. The phase difference between wavefronts $\Delta(A')$ in the region of point A' (respectively, A_1' and A_2'), is the optical path difference between point A (respectively, A_1' and A_2') and its background, represented in Fig. 3 A as Δ_{obj}. This phase difference, Δ_{obj}, can be measured precisely with the image-duplication instrument (BARER, 1952; DAVIES, WILKINS, 1952; ROSS, 1967). Now, if we add a bias retardation ($\Delta_b \neq 0$, Fig. 3 B), by any kind of compensation (e. g. DE SÉNARMONT or EHRINGHAUS, or by tilting the auxiliary calcite plate of the condenser), we can vary contrast at will, yet the wavefronts remain just as laterally separated in the region of the objects as when the background was at extinction. The phase difference between the interfering wavefronts in terms of the object (see Eq. (1)) can be expressed as:

$$\Delta(A') \equiv \Delta_{obj} + \Delta_b . \tag{2}$$

Therefore, the intensity of the beam emerging from the analyser, in the region of the object (I_{obj}) is:

$$I_{obj} = I_{max} \sin^2 \tfrac{1}{2} (\Delta_{obj} + \Delta_b) + I_{min} . \tag{3}$$

Further, there is no lateral overlap at any azimuth, so that the emergent beam has precisely the same intensity along azimuths *AO*, *BO* and *CO* (Fig. 2).

Fig. 4 A—I, represents the corresponding sheared wavefronts (Σ_1' and Σ_2') obtained with the differential interference equipment, for the object drawn in Fig. 2, but now 2 μm in diameter. Wavefronts Σ_1' and Σ_2' interfere in precisely the same way as in the image-duplication instrument, and the intensity at any point of the emergent beam is once again a function of the phase-difference between the wavefronts at that point, $\Delta(A')$ (see Eq. (1)). However, there is now an important difference. The distance of shear is very small (about 0.2 μm with the 100/1.25 oil-immersion objective) in relation to the dimensions of the object, and therefore in the differential system there always is a substantial lateral overlap between the wavefronts. In Fig. 4 A—C, the interfering wavefronts correspond to a zero bias retardation or extinction (adjusted by turning the micrometer screw of the beam-splitter). At A we have the wavefronts corresponding to azimuth *AO* of Fig. 2 (parallel to the direction of shear). In the differential system the phase difference between the sheared wavefronts no longer corresponds to the phase difference between points in the optical object and the object surround (Eq. (2)), but to the gradient in phase difference across the optical object:

$$\Delta(A') \equiv a \frac{\partial}{\partial x} \Delta_{obj}(A') + \Delta_b \tag{4}$$

and therefore:

$$I_{obj} = I_{max} \sin^2 \tfrac{1}{2} \left[a \frac{\partial}{\partial x} \Delta_{obj}(A') + \Delta_b \right] + I_{min} , \tag{5}$$

where a is the effective lateral shear in the plane of the object, and x is the direction of shear (direction *XX* in Fig. 2).

At extinction (Fig. 4, A and B), there is no phase difference between the wavefronts in the background, and where the sheared wavefronts intersect. These regions would appear uniformly dark ($\Delta_b = 0$, $\Delta(A') = 0$, $I = I_{min}$, Eqs. (1), (3), and (5)), flanked by two regions of equal brightness having intensity peaks at A_1' and A_2' at a distance a

from each other. However, one slope of each partially sheared wavefront is now phase-advancing in relation to the background region, and the other is phase-retarding. Therefore, after adding a bias retardation, Δ_b, one slope would be brightened and the other darkened, producing the shadow-cast effect.

Considering azimuths *BO* and *CO* (Fig. 4 B, C), we see that, because of the lateral overlap of the sheared wavefronts, the effective lateral separation between wavefronts, in the direction of shear, becomes progressively smaller at azimuths making increasing angles β with the direction of shear, and it reaches zero at right angles (azimuth *CO*, Fig. 4 C). This property becomes readily understandable by considering what happens to the globule in the image plane (Fig. 5). For $\beta = 90°$, no interference contrast is generated. For any particular azimuth, the effective lateral separation between wavefronts is the lateral separation in the direction of shear, multiplied by the cosine of the angle β, made by that azimuth with the direction of shear.

To exploit the "optical shadow-casting" possibilities to the full, it is necessary to use bias compensation rationally. In Fig. 4 D—F, we see the effects of adding a small amount of background retardation. Along the azimuth parallel to the direction of

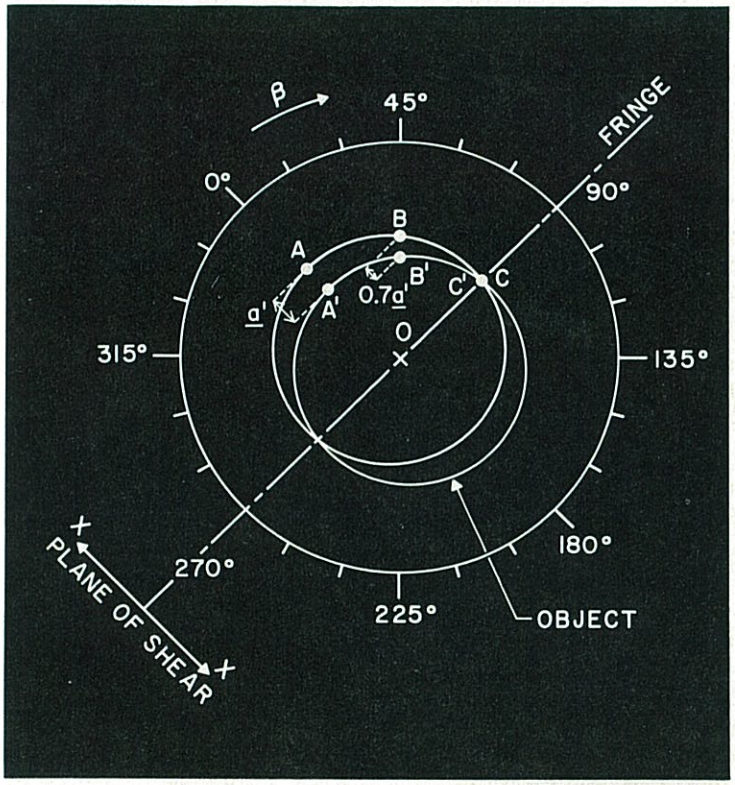

Fig. 5. Diagrammatic representation of a flattened spheroid (see Fig. 2), but now 2 μm in diameter, as it might appear in the field of a differential interference microscope. This diagram is related to Fig. 4 thus; if we section Fig. 5 along azimuths *AO*, *BO* and *CO*, we obtain the elevations or profiles drawn in Fig. 4 A—C. Fig. 5 illustrates how the overlap between wavefronts produces a variable shear, in the direction of shear, *XX*, for points *A*, *B* and *C*. See text and Figs. 2—4.

shear, AO, $\beta = 0°$ (Fig. 4 D), there now is a complete superimposition of the sheared wavefronts along the trailing edge of the optical object (or southeastern region of azimuth AO). The phase difference in this region is zero, and so is the resultant light intensity. The phase difference between wavefronts along the opposite slope is emphasized, hence producing an intensity gradient between the leading and trailing edges of the optical object in the direction of shear; and the background intensity is intermediate between these. Along an azimuth at right angles to the direction of shear, CO (Fig. 4 F), no differential interference contrast is generated, and the intensity is that of the background. The object would appear as though illuminated obliquely by a source northwest of A. It should be noted that, for any optical object, either slope can be made to merge with its sheared portion, depending on the sign of the bias compensation added. Further, slopes can be made to merge at any azimuth, by rotation of the object and suitable adjustment of the bias compensator, as shown in Fig. 4 G—I. The degree of bias compensation required to darken maximally one slope of an optical object is also the correct setting for obtaining the maximum possible contrast between that object and its surround.

Operational principles

The principles of operation of the differential interference microscope equipment can be summarized in a set of postulates derived from the analysis given above.

Postulate I. The optical property of a microscopic object that generates differential interference contrast is the gradient of phase difference across the object in the direction of shear; the optical object is perceived by its slopes.

Therefore, in the generation of differential interference contrast, the geometrical configuration of the object is a more important property than the absolute phase shift produced by it. Steep gradients in phase difference (e. g. refractive interfaces, such as those defined by the membranes, filaments, and edges of globules and vacuoles, that characterize biological objects) are emphasized, and they appear in sharp contrast to their background; gentle slopes, even when they introduce quite large absolute optical path differences, are minimized, and they may generate little or no interference contrast. This property is illustrated in Figs. 6 – 8. Fig. 6 represents the diatom *Stauroneis acuta*, photographed under the Zeiss

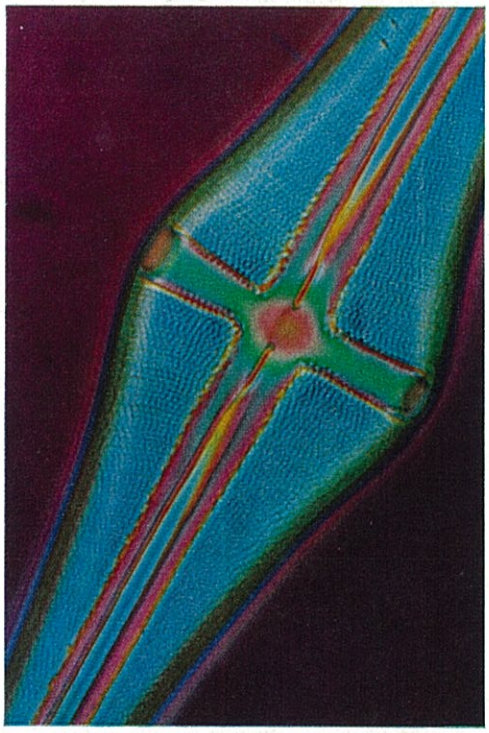

Fig. 6. Diatom *Stauroneis acuta*, Zeiss image-duplication interference microscope equipment II, 40/0.65 $\Delta_b = +551$ nm. Compare with Fig. 7.

image-duplication interference equipment 40/0.65 (PILLER, 1962). From the interference colour-contours, we see that there is an absolute optical path difference of about $2^1/_4\ \lambda$ between the centre of the frustule and the immersion medium. When the same object is photographed under the Zeiss/Nomarski differential interference equipment 40/0.65 (Fig. 7), we see that this large but gradual phase difference does not

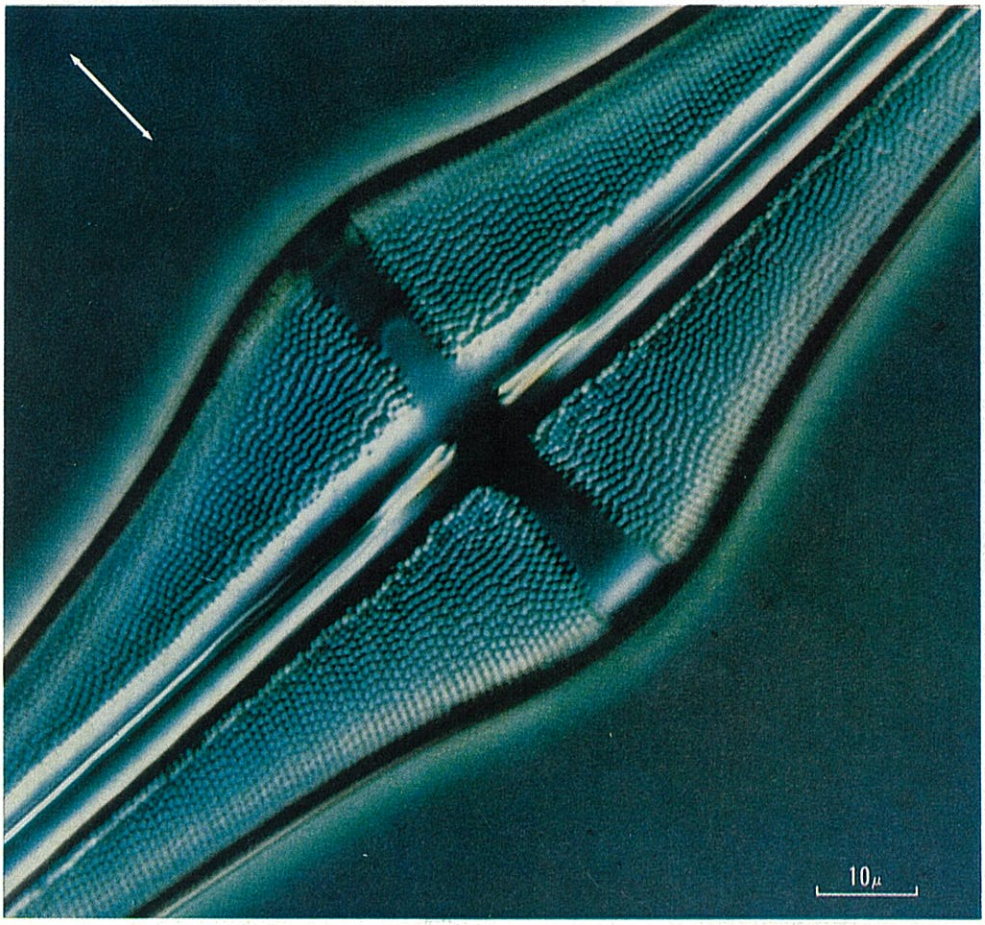

Fig. 7. Diatom *Stauroneis acuta* (same specimen as in Fig. 6), Zeiss/Nomarski differential interference equipment 40/0.65. $\Delta_b \cong +91$ nm. The arrow indicates the direction of shear. Compare with Fig. 6.

contribute significantly to differential interference contrast: only the steep gradients of the valve details are emphasized. Finally, in Fig. 8, we have one of the most difficult of all biological objects, photographed under the Zeiss/Nomarski differential equipment 100/1.25: a living dividing cell of the African bloodlily *Haemanthus katherinae*, showing quite clearly the tenuous spindle fibre filaments (BAJER, ALLEN, 1966 a and 1966 b). These filaments cannot be seen clearly by other methods of optical microscopy applicable to the study of living cells.

Postulate II. Contrast varies proportionately with the cosine of the angle made by the azimuth of the object with the direction of shear.

The most spectacular demonstration of this principle is afforded by essentially unidimensional structures. Fig. 9 A, B, illustrates the diatom *Hantzschia amphioxys*, photographed under the Zeiss/Nomarski differential interference equipment, 100/1.25.

Fig. 8. *Haemanthus katherinae*, endosperm cell, in metaphase. Zeiss/Nomarski differential interference equipment 100/1.25.

In Fig. 9 A, the long axis of the diatom was oriented at 90° to the direction of shear (large arrow); in B, parallel. This diatom has surface ridges oriented at 90° to its long axis, studded with cortical fenestrations about 0.18 μm in diameter (small arrows in A). The cortical fenestrations are clearly visible in A, but not the larger ridges; the ridges are beautifully sharp in B, but not the fenestrations. Because of this, it is important to examine unknown objects at several azimuths, and to indicate the direction of shear in all differential interference micrographs. The azimuth effect is equally obvious in radially symmetrical objects, such as the diatom *Arachnodiscus ehrenbergi* (Fig. 10), here photographed under the Zeiss/Nomarski system 100/1.25.

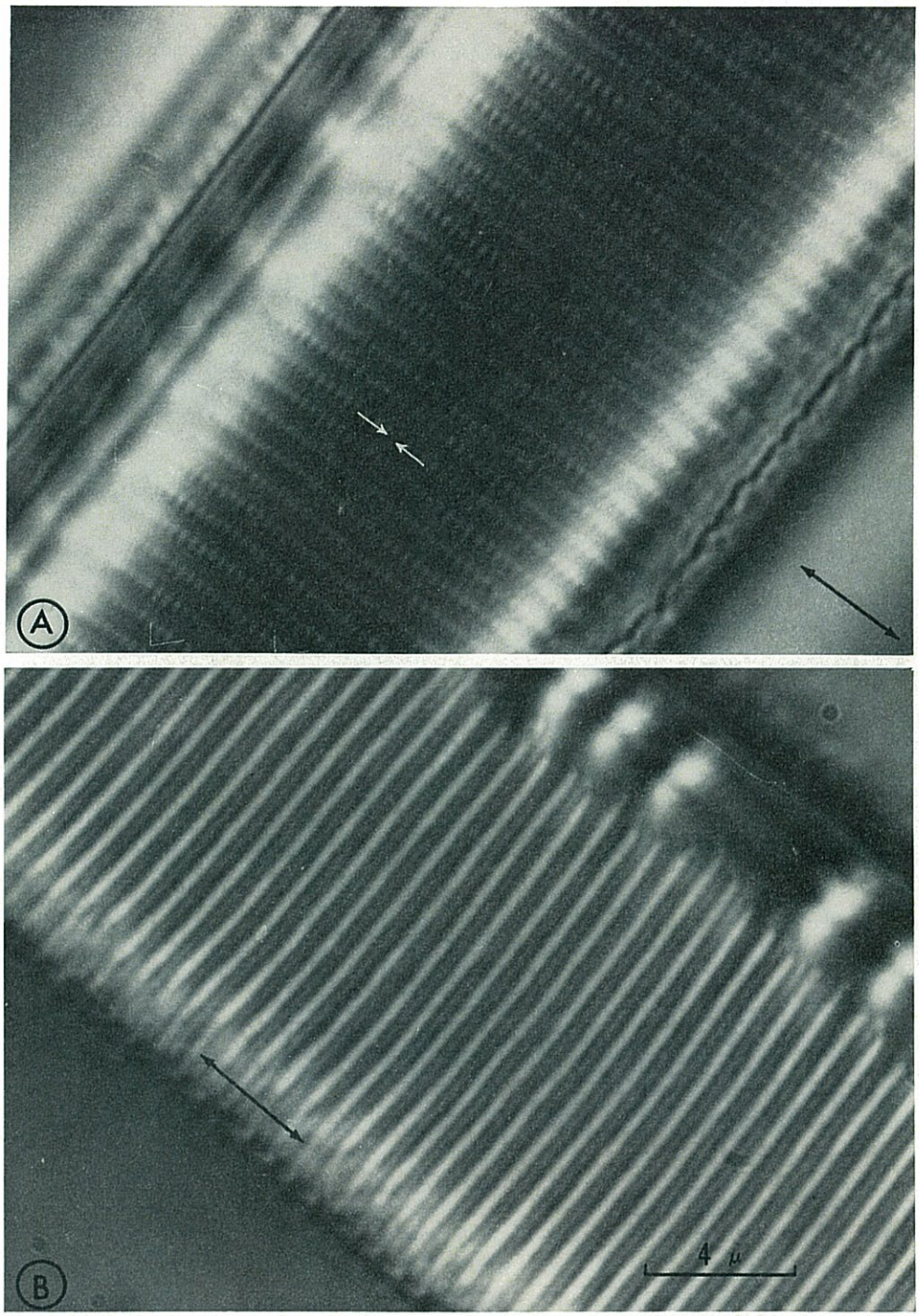

Fig. 9. Diatom *Hantzschia amphioxys*, Zeiss/Nomarski differential interference equipment 100/1.25, with the long axis of the diatom oriented perpendicular (A) and parallel (B) to the direction of shear (indicated by the large arrows). A and B represent two images of precisely the same area of a diatom, photographed at the same focal plane; the only instrumental difference between them is that the microscope stage was rotated 90° between exposures.

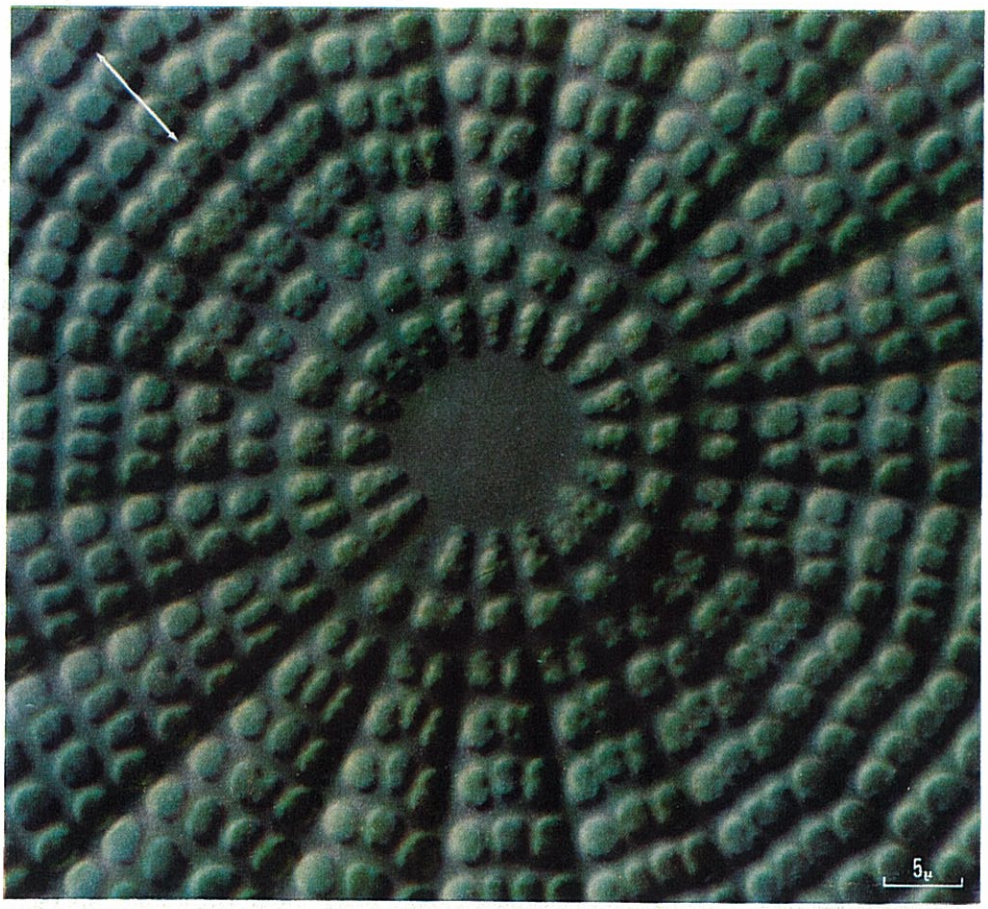

Fig. 10. Diatom *Arachnodiscus ehrenbergi*, Zeiss/Nomarski differential interference equipment 100/1.25. The arrow indicates the direction of shear.

Postulate III. The "optical shadow-casting" effect is emphasized when one slope of the optical object in the direction of shear is brought to extinction by the use of bias compensation (Fig. 4 D). This instrumental setting will also yield the highest possible contrast and the most faithful geometrical image of the optical object.

It will readily be appreciated (see Fig. 4) that at instrumental extinction the optical object appears bisected by a dark line; at this setting a very small object could appear doubled, and geometrical measurements of extended objects might be exaggerated in the direction of shear. As bias retardation is added or subtracted, the dark line will move toward one or the other edge of the optical object. If the bias retardation (of either sign) is greater than that necessary to produce the "shadow-cast" effect, the resulting contrast is reduced.

Postulate IV. Gradients of phase difference of opposite sign produce shadows in opposite directions.

The direction of a particular shadow is purely arbitrary, and can be reversed at will. It is convenient to set the bias compensator so as to follow the traditions of artistic perspective, and to have phase-retarding object details (more refractile than their surround) appear as though in high-relief, and phase-advancing details (less refractile than their surround), as though in bas-relief. "Shadows" should then appear as though "cast by the setting sun". These useful optical illusions are illustrated in Fig. 11, a micrograph of a living and dividing cell of *Haemanthus*

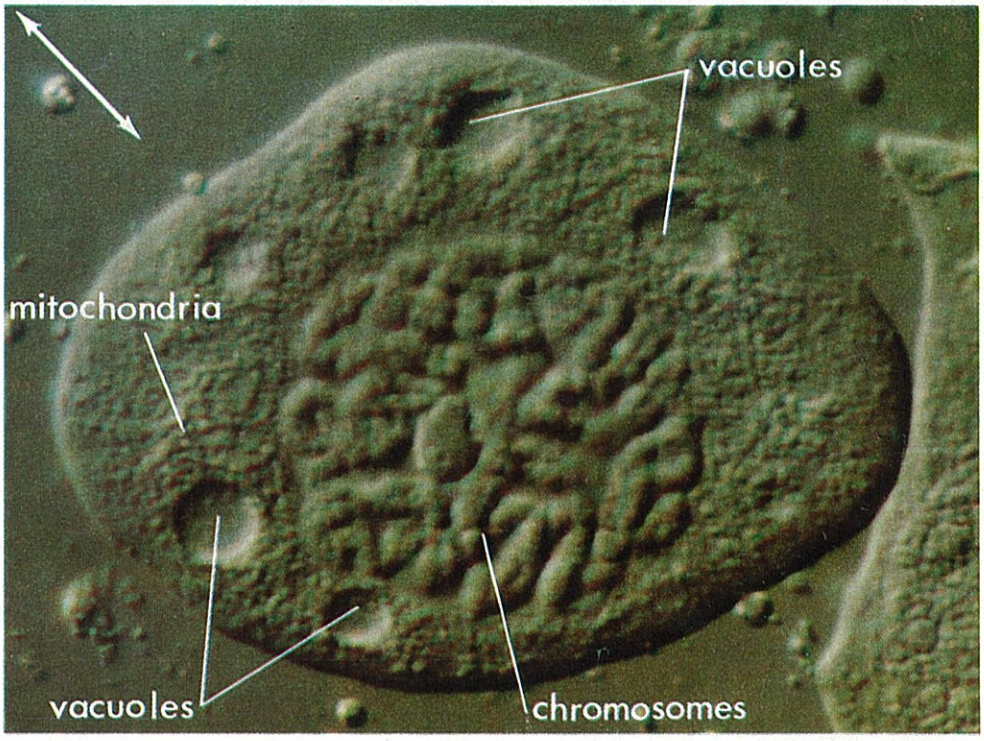

Fig. 11. Endosperm cell of *Haemanthus katherinae*, Zeiss/Nomarski differential interference equipment 100/1.25; bias retardation adjusted so as to darken maximally the lower right edge of the cell (see Fig. 4 D). The arrow indicates the direction of shear.

katherinae, photographed with the Zeiss/Nomarski differential system 100/1.25. Note that the large water-filled vacuoles (of low refractive index, and hence phase-advancing relative to their surrounding cytoplasm) have "shadows" cast in the direction opposite from that in the cell itself and in all other sub-cellular structures (mitochondria, chromosomes, etc.), which are phase-retarding relative to their immediate surround. A complete reversal of the direction of the shadows is obtained if the sign of the bias compensation is changed (by turning the compensator screw in the opposite direction, past extinction), or if the differential interference micrograph is printed in reverse. The "shadow-cast" effect is useful, for it provides unequivocal information about the refractive properties of object details, but this should not be mistaken for true stereoscopic representation.

Postulate V. In the case of thick or highly light-scattering objects, the optimal contrast may be reached at a bias compensator setting somewhat higher than the extinction setting for one slope of the optical object (cf. Postulate III).

As the bias compensation is increased, the ratio of scattered to transmitted light decreases. We have observed the benefit of working at high compensator settings in observing or recording details of cell structure in cultured ganglia which present significant amounts of light scattering above and below the plane of the object of interest.

Contrast and resolution

The sensitivity of an optical instrument is limited by the stray light produced in it. The amount of stray light ultimately depends on such factors as the degree of coherence of the interfering wavefronts, which is influenced by the effective geometry of the light source, the number and kind of refractive interfaces in the optical system, strain in the optical components, and the perfection of the superimposition of the fringes of the two modified Wollaston prisms. Such optical properties of the microscopic object as light-scatter may also redistribute some light over the image plane.

The degradation of contrast due to instrumental stray light in the differential interference system (or any other polarizing instrument) can be estimated from the instrumental extinction factor (SWANN, MITCHISON, 1950; INOUÉ, 1952). This is defined as the ratio of the maximum and minimum light intensities transmitted by the complete microscope under operational conditions, respectively, at maximum constructive and destructive interference. The extinction factor sets the limit of the minimum signal that can be detected against a background of noise as stray light. With the Zeiss/Nomarski system, values for the extinction factor of 100 to 1,000 are routinely obtained, depending on the condenser aperture, the individual objective, beam-splitter and compensator used. This range is 1 to 2 orders of magnitude higher than that obtainable with image-duplication interference microscopes, and it permits the detection in differential interference micrographs of gradients in phase difference as small as 3×10^{-3} radians, at a signal-to-noise-ratio of 2, in fine-grain interference micrographs. Further, for any particular objective, the extinction factor remains high until the condenser aperture exceeds about 3/4 of the objective aperture. Therefore, it is possible to obtain at the same time both high contrast and high resolution. Figs. 12 and 13 are photomicrographs of the diatom *Surirella robusta* taken with different optical combinations to illustrate this effect. Fig. 12 A, was photographed at nearly full aperture with the Zeiss/Nomarski differential system 100/1.25; for Fig. 12 B, the same system was used, but with the condenser stopped down to an aperture of 0.6. The contrast in Fig. 12 A, is nearly as high as that in Fig. 12 B. For comparison purposes, Fig. 13 A, was photographed by phase-contrast microscopy (Planapochromat objective Ph 100/1.3) and 13 B, by direct microscopy (Planapochromat objective 100/1.3).

The limit of spatial resolution for an optical system having a given aperture, set by diffraction due to the wave nature of light, was first formulated by ABBE nearly a century ago (1910). In modern analytical terms, the optical system transfers a limited

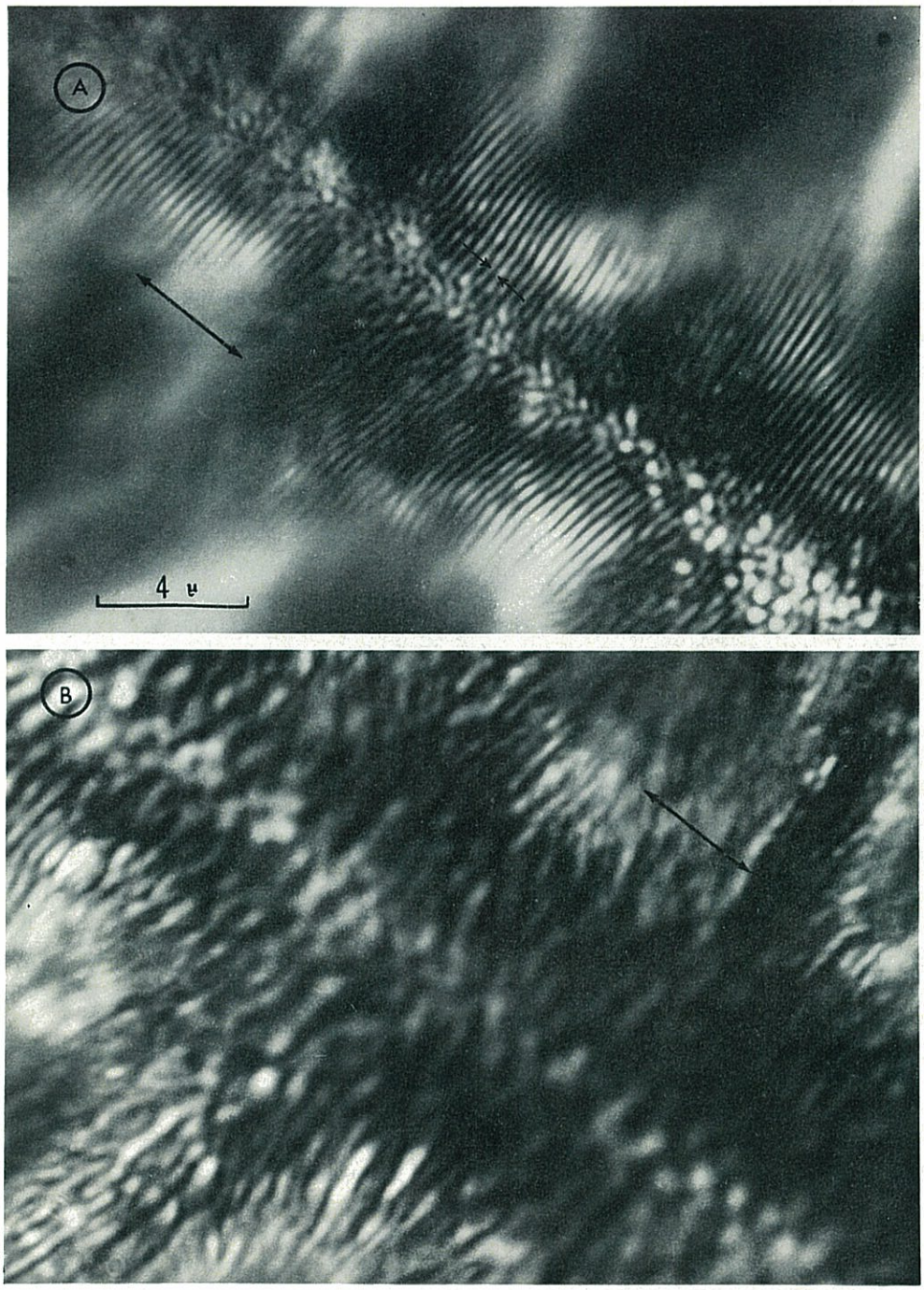

Fig. 12. Diatom *Surirella robusta*, Zeiss/Nomarski differential interference equipment 100/1.25. At A, the condenser was opened to nearly full aperture; and it was stopped down to 0.6 for B, care being taken not to alter the focus between them. Both micrographs were processed together, and they were printed at the same magnification on paper of the same contrast. The small arrows at A indicate the fine striations of this diatom (about 0.1 μm thick, repeat-period 4,500/mm). These striations only become clearly visible when the condenser aperture approaches that of the objective. The large arrows indicate the direction of shear.

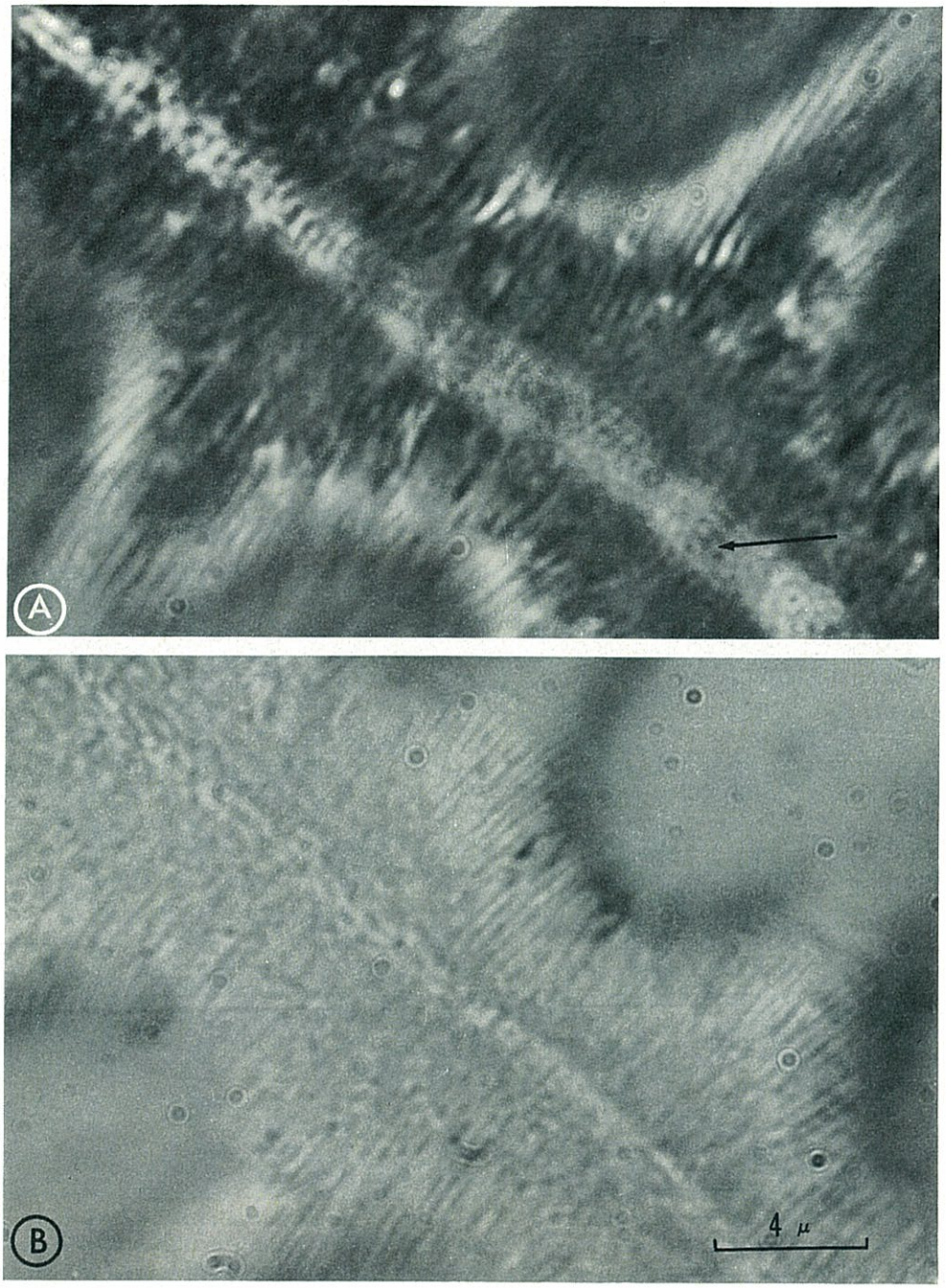

Fig. 13. Diatom *Surirella robusta*, same field as in Fig. 12, photographed at the same focal plane and magnification under A, Zeiss Planapochromat 100/1.3-Ph, positive phase-contrast system, and B, Zeiss Planapochromat 100/1.3 bright-ground system, on-axis, and at a slightly reduced condenser aperture. Note the 'granularity artifact' in the phase-contrast system (arrow at A), and the generally poor contrast of both systems when compared with Fig. 12.

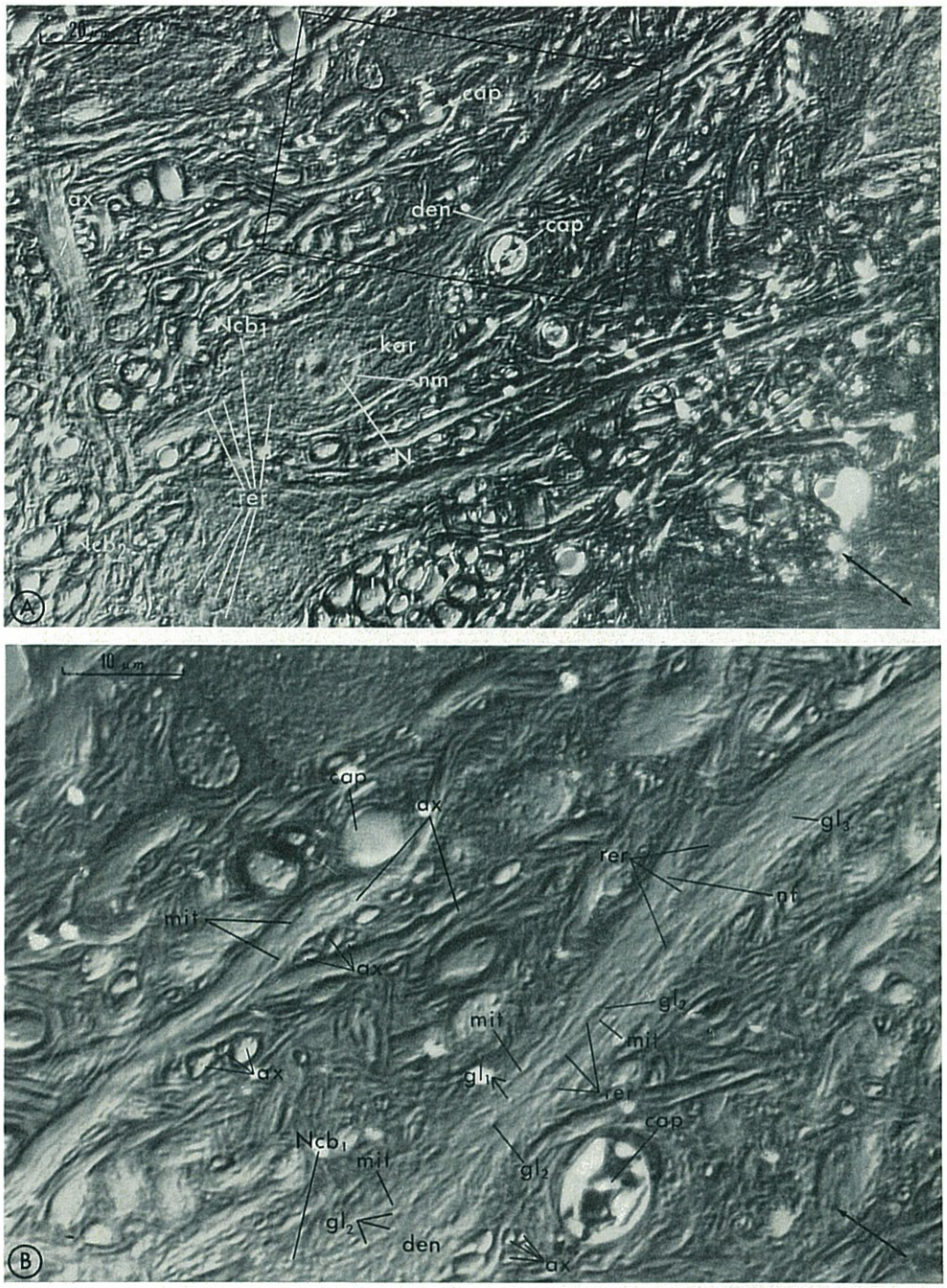

Fig. 14. Unstained 3.5 μm section through a cranial motor nerve nucleus of the brain-stem of the rat, fixed in glutaraldehyde, post-osmicated, and embedded in Epon. The direction of shear is indicated by the arrows. A was photographed under the Zeiss/Nomarski differential interference equipment 40/0.85, and B under the 100/1.25 equipment. B represents the rectangular area outlined in the survey-photograph A. Abbreviations: *ax*, axons (both in longitudinal and cross-section); *cap*, capillaries; *den*, dendrites; gl_1, globules, about 0.5 μm in diameter, apparently distributed at random within the cytoplasm of neurones; gl_2, globules, 0.2—0.3 μm in diameter, frequently found in rows oriented parallel to mitochondria and filamentous material; gl_3, minute globules <0.1 μm in diameter, widely distributed; *kar*, karyosomes; *mit*, mitochondria; *N*, nucleus; Ncb_1, Ncb_2, cell bodies of two neurones; *nf*, filamentous material (bundles of a few microtubules?), <0.1 μm in diameter; *nm*, nuclear membrane; *rer*, rough endoplasmic reticulum (Nissl complex) within neuronal cell bodies and dendrites.

band of spatial frequencies from the object plane to the image plane; the bandwidth and the cut-off frequency are determined by the angular aperture of the system, and the wavelength of the light used. Ordinarily, the cut-off frequency (R) for periodic objects is of the order of $2\,\text{N.A.}/\lambda$ for an objective (where N.A. is the numerical aperture of the objective, and λ the wavelength). This value corresponds to a theoretical resolution limit of about 4,500 lines/mm or 0.22 μm repeat-period ($1/R$) for an oil-immersion objective 100/1.25, using green light of 550 nm. Theoretically, in ordinary bright-ground microscopy, object details with spatial frequencies approaching the diffraction limit (or cut-off frequency), are imaged with negligible contrast. Practically, glare in bright-ground systems substantially narrows the available bandwidth by reducing contrast at high apertures; glare can be reduced and contrast increased by stopping down the condenser aperture: stopping down the aperture necessarily leads to a reduction in the resolution obtainable with the microscope system under operational conditions. As we have seen, the Zeiss/Nomarski differential interference system is inherently a low-glare instrument: it is not necessary to stop down the condenser aperture in order to secure high contrast. A tangible gain in obtainable resolution is thereby achieved. A further gain is obtained through spatial filtration. Wollaston prisms producing shear of the order of magnitude of the diffraction limit in the object plane, act as spatial filters, emphasizing high spatial frequencies, and attenuating lower frequencies. In the Zeiss/Nomarski differential interference equipment, optical objects with details at the ordinary cut-off frequency oriented parallel to the direction of shear, are imaged with little loss of contrast. This is clearly seen in Figs. 12 A, and 13. The striations of this diatom form a grating of approximately 4,500 lines/mm (each dark striation is approximately 0.1 μm wide). Neither phase-contrast nor bright-ground microscopy (Fig. 13 A and B) approaches this degree of resolution. Further, the differential interference image (Fig. 12 A) is singularly free of the "granularity artifact" due to unsuitable spatial filtration (DAVID, 1964), and spurious contrast due to out-of-focus details, which are only too evident in the equivalent phase-contrast image (Fig. 13 A).

The usefulness of the improved contrast and resolution of the Zeiss/Nomarski differential interference system in practical cytology is self-evident. A wealth of unsuspected detail becomes visible even in "difficult" materials. An example will suffice (Fig. 14), survey and high-resolution differential interference micrographs of a section of rat brain-tissue, processed for subsequent electron microscopy, but cut at 3.5 μm.

Depth of field and optical sectioning

Because the Zeiss/Nomarski differential interference equipment can be used effectively at large condenser apertures, the depth of field is inherently shallow. There is in the differential interference microscope another consequence of the combined effects of shearing of wavefronts and the use of high numerical aperture illumination: object details lying more than about 3 Airy disc radii above or below the plane of focus of the objective do not materially contribute to the generation of contrast. This results in an exceptional freedom from spurious contrast, particularly in

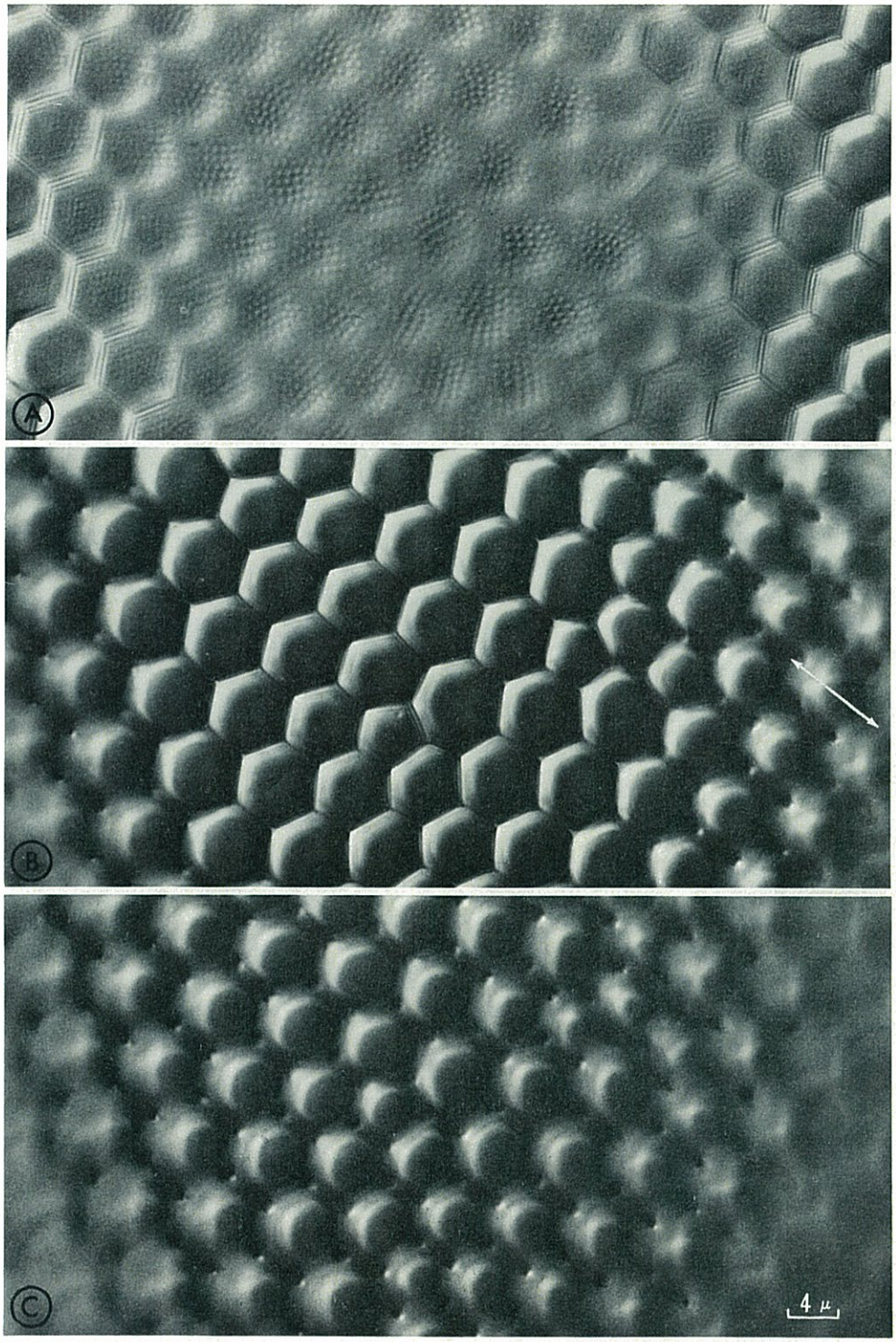

Fig. 15. Diatom *Triceratium favus*, Zeiss/Nomarski differential interference equipment 100/1.25. These are three photographs of a focal series; *A* was focused on the cortical fenestrations, *B* and *C* at successively greater depths. The arrow indicates the direction of shear for the three micrographs. Compare with Fig. 16.

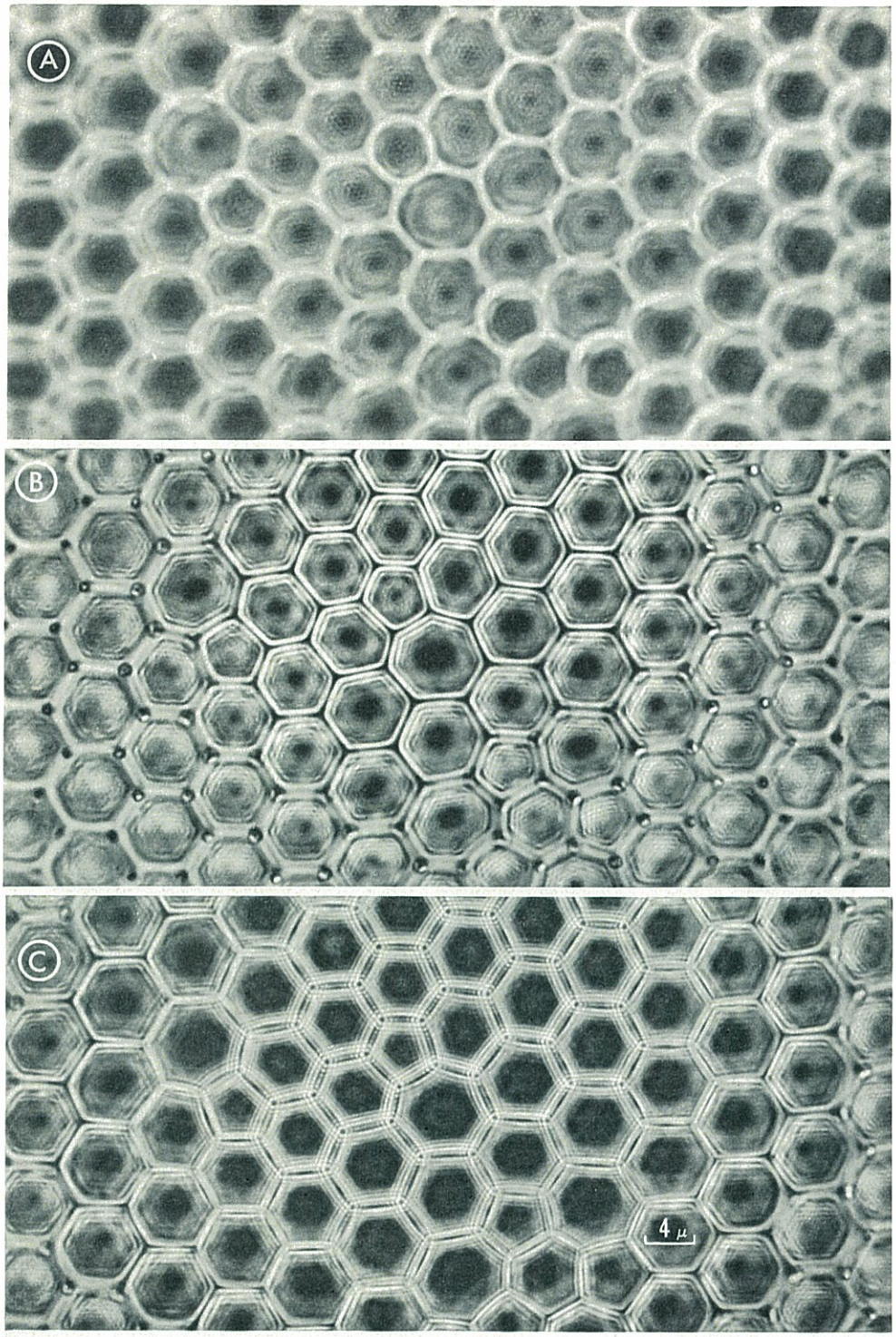

Fig. 16. Diatom *Triceratium favus*, Zeiss/Planapochromat positive phase-contrast equipment 100/1.3-Ph, same fields as in Fig. 15. Compare 15 *A* with 16 *A*, 15 *B* with 16 *B*, etc. Note the poor contrast of the cortical fenestrations in 16 *A*, and the very curious diffraction artifacts throughout the focal series.

comparison with phase-contrast microscopy. An example is given in Figs. 15 and 16. These are micrographs of three closely adjacent focal planes of the diatom *Triceratium favus*, under the Zeiss/Nomarski differential equipment 100/1.25 (Fig. 15), and the 100/1.3 Planapochromat-Ph phase-contrast equipment (Fig. 16). Note that the cortical fenestrations that are so clearly seen in the differential interference micrographs (Fig. 15 A) are almost completely obscured by out-of-focus details in the corresponding phase-contrast image (Fig. 16 A). Further, annular diffraction images prevent the accurate geometrical representation of object details much below the surface in the phase-contrast micrographs (Fig. 16 B—C).

This capacity for efficient optical sectioning of thick objects is one of the most important advantages of differential interference microscopy in biology and medicine. L i v i n g objects ranging from bacterial cells and protists to whole small invertebrates, organotypic tissue cultures, and small embryos of larger animals can be examined under favourable biological conditions without interfering with their normal life processes, and at a resolution surpassed only by electron microscopy. Several differential interference cinémicrographic films of these subjects were produced in our laboratories (and published by the Ealing Corporation, 2225 Massachusetts Avenue, Cambridge, Mass., USA). In one of these, made in collaboration with Dr. J. GILBERT and shown at the London Centenary Conference of the Royal Microscopical Society, the rotifer *Asplanchna sieboldi* was optically dissected. The relative positions of the internal organs were filmed under the 16/0.32 system; then the histological details

Fig. 17. Living *Asplanchna sieboldi* rotifer, stomach with bolus within it, and two digestive glands. Zeiss/Nomarski differential interference equipment 100/1.25. The arrow indicates the direction of shear. See text.

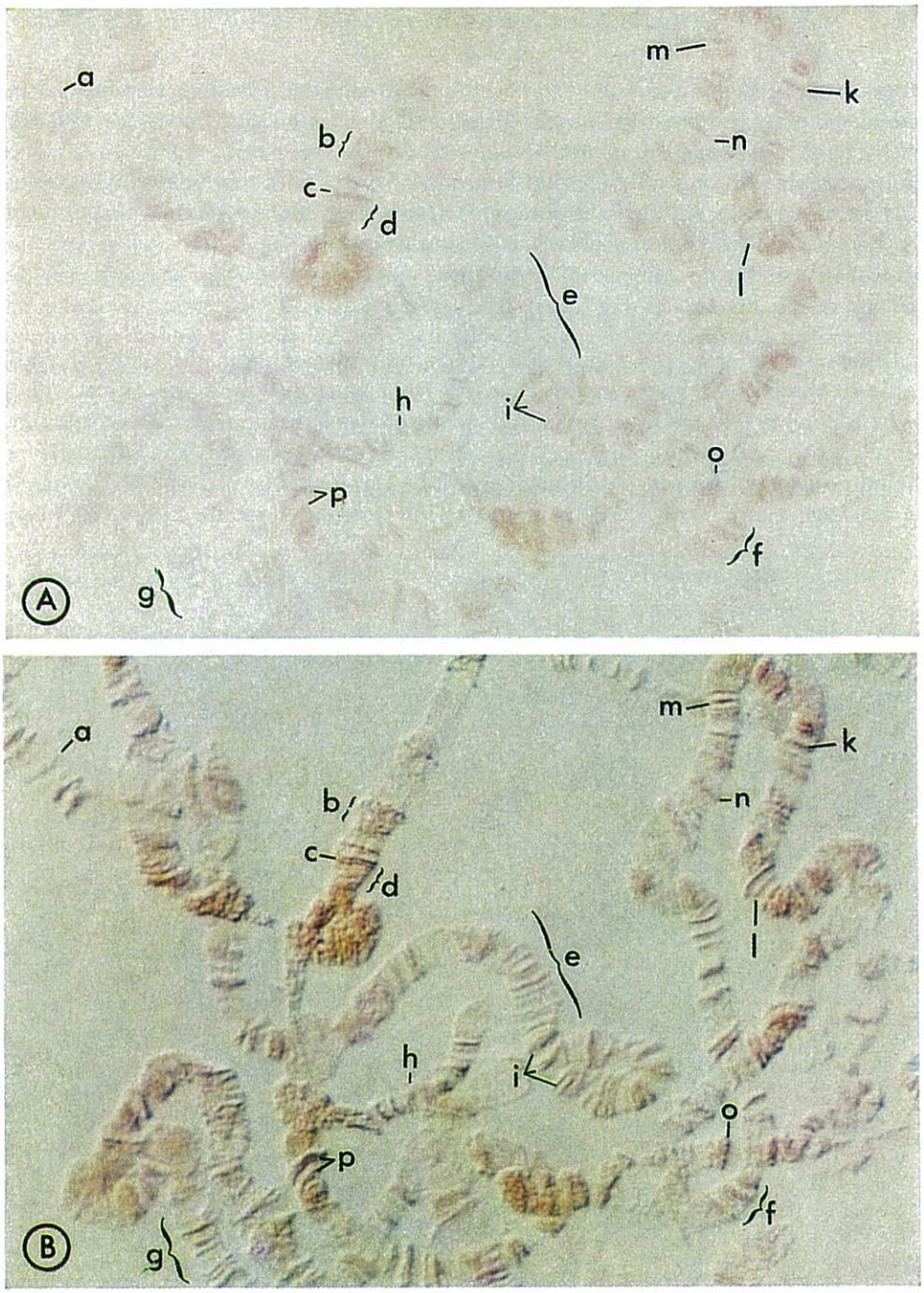

Fig. 18. Chromosome smear of *Drosophila melanogaster*, weakly stained in aceto-orcein. A, bright-ground microscopy, Zeiss Planachromat 100/1.25, at full aperture. B, Zeiss/Nomarski differential interference equipment 100/1.25, with both phase and amplitude compensation, at full aperture. Compare *a* with *a*, *b* with *b*, etc. The amplitude contrast arrangement permits the resolution of approximately twice as many bands as the bright-ground microscopy system. Further, c o i l e d bands can be seen for the first time.

within organs, under the 40/0.65 system; and finally the detailed structure of individual neurones, contracting muscle fibres, and glandular cells, under the 100/1.25 oil-immersion system. The contrast and resolution in these cells, examined within an intact living organism 0.5-mm thick, are comparable with those that might reasonably be expected in a thin tissue culture. A frame from the *Asplanchna* film, showing the stomach and two digestive glands, is illustrated in Fig. 17.

Amplitude contrast

Differential interference microscopy has become invaluable in the study of "difficult" absorbing objects, irrespective of whether they also are phase objects. These include chloroplasts in living protists, pigment globules in living metazoan cells, stained chromosome spreads, and thin, weakly-stained microtome sections. The adjustment of the microscope to compensate absorption will be considered here. For high contrast to be achieved in any form of microscopy using interference effects the interfering beams

Fig. 19. Chromosome smear of cultured normal human peripheral lymphocyte, stained in aceto-orcein, and photographed in amplitude contrast under the 100/1.30 Planopochromat-Zeiss/Nomarski differential interference contrast equipment. Note the coiling of he chromosomes (pitch about 0.4 μm) and the granular internal detail. (smear: M. Lejeune, micrograph: Institut d'Optique/Paris.)

must have approximately the same amplitude. For either weakly absorbing or highly refractile objects, a satisfactory match of their relative amplitudes may be impossible. In the differential interference equipment, as well as in image-duplication systems (KOESTER, OSTERBERG, WILLMAN, 1960), it is possible to vary the relative amplitudes of the interfering beams at will, simply by rotating the substage polarizer a few degrees. In practice, bias retardation is adjusted to produce the optimum shadow-cast effect, and then the polarizer is rotated in one of the two directions until the edge of the absorbing detail appears maximally dark. The amount of rotation of the polarizer required to achieve this depends on the amplitude gradient across the object. If one works in white light, these compensation procedures do not affect the spectral absorption of the object details, which are then perceived in vivid colour contrast and with increased resolution. This is illustrated in Fig. 18, a squash of the giant chromosomes of the salivary glands of *Drosophila melanogaster*, stained in aceto-orcein and photographed under the 100/1.25 Zeiss/Nomarski equipment.

One field in which the amplitude contrast effect obtained with the Zeiss/Nomarski interference microscope equipment may well supplant other methods of examination is in the karyotyping of human chromosomes. The freedom from glare, enhanced contrast of absorbing details, and increased resolution of the differential system make it possible for the first time to begin to study meaningfully the morphological details of the internal structure of human chromosomes. An example of what can be achieved is given in Fig. 19.

Practical suggestions to users

1. The microscope should always be adjusted to obtain the highest possible extinction factor. A sensitive photoelectric photometer should always be used to measure the extinction factor under operational conditions. The measurement should be carried out with the microscope fully set up, and the microscopic specimen moved a little to one side, so as to leave a clear field. The minimum intensity should be measured at instrumental extinction, and the maximum intensity after π radians bias compensation is introduced. Extinction factors below 100 are considered to be unacceptable in our work and for careful work we prefer to use extinction factors in excess of 200.

2. The optical components, microscopic object, specimen-chamber, and coverglass must all be extremely clean. Care to avoid contaminants should be exercised when mounting the specimen, and chemically clean strain-free chambers and coverglasses should be used. Optical components should be degreased with ether, and dust is best dispersed by a jet of filtered air or freon. Dirt is the most common cause of poor results.

3. The top lens of the condenser must always be oiled to the under-surface of the slide or specimen chamber, to reduce glare. This step eliminates the most awkward refractive interface in the system.

4. The precision of superimposition of the fringes of the two Wollastons (hence cancelling-out of their retardations) is critical in maintaining the coherence of the interfering wavefronts. Superimposition is only possible if lower Wollastons of the

correct size and crystal orientation (check designations) are at the right height to be imaged in the plane of the fringes of the beam-splitter by the condenser and objective. This is best achieved by KÖHLER illumination. Proceed thus:

a) Focus the object as sharply as possible.

b) Adjust the height of the condenser so that the field stop is focused in the object plane.

c) Adjust the lamp collector so that the actual source (preferably the HBO 200, or other high-pressure arc) is focused in the plane of the condenser aperture stop and completely fills the aperture.

d) If the microscope is equipped with a pre-centred ball-bearing Pol stage and objectives mounted in single centring objective-changers, centre the optical train thus:

(i) Find the centre of rotation of the stage, and bring a recognizable object detail to it with the x and y movements of the mechanical stage.

(ii) Bring this object detail to the centre of the field of view (eyepiece cross-lines!), by means of the objective-centring keys.

(iii) Centre the field stop with the centring screws of the substage mount. Open the field stop only to the edge of the field.

(iv) Examine the exit pupil of the objective with the BERTRAND lens (Optovar or Pol tube fitting). Open the aperture stop completely. Darken the exit pupil maximally by slowly adjusting the bias compensator, until the dark (zero order) fringe nearly fills the aperture. If the dark fringe substantially fails to fill the exit pupil, readjust the height of the condenser, even if the field-stop then becomes slightly defocused.

(v) Partly close the aperture stop. Centre it to the dark region of the exit pupil, with the two small levers on the condenser mount. Open the aperture stop so that about 3/4 of the objective exit pupil is filled. Return to orthoscopic conditions.

e) If the microscope is equipped with a centring stage and a non-centring objective nose-piece, instead of d) (ii), above use the stage centring keys to bring the object into the centre of the field of view.

f) When focusing through thick objects, always re-adjust the condenser height, so that the field stop remains focused in the object plane.

5. With the bias compensator set at extinction, adjust the polarizer so that it is crossed with the analyzer.

6. Set the best bias compensation. Beginning at instrumental extinction, carefully adjust bias retardation, so that the lower right edge of the object detail under examination (if it is phase-retarding) is maximally darkened (upper left edge, if phase-advancing). Always rotate the object, examine several azimuths, and constantly vary the bias retardation. No single setting is ideal for all details in any objects.

7. Compensate absorption due to the microscopic object by slightly rotating the polarizer in one of the two directions, if necessary.

8. Colour contrast or brightness contrast? When mixed phase-amplitude objects are being examined, it is best to use white light (e. g. the unfiltered xenon arc XBO 150), and bias compensation near extinction. When phase objects with very large gradients are under consideration (in which high contrast is not a problem), it is largely immaterial whether Order I interference colours are used in white light or

not. But for all other objects — the vast majority of the situations likely to be encountered in biomedical work — image quality is enhanced by using nearly monochromatic light of 546 nm (HBO 200 mercury arc and PIL 546 precision line interference filter), and bias compensation near extinction.

9. Finally, a word about photographic technique. The differential interference image, in a well-adjusted system of high extinction, is necessarily of low luminance — even when an intense source is used. Contrast nuances are not well perceived by the eye under scotopic or even mesopic vision. Many object details become apparent for the first time only when enlarged differential interference micrographs are examined: this situation is comparable to that existing in electron microscopy.

For differential interference micrography in monochromatic light of 546 nm, we found that the most satisfactory results were obtained with comparatively slow photographic emulsions of fine-grain and high-acutance, such as Adox KB14 for 35-mm photography, and Kodak (U.K.) High-Contrast Pan for 16-mm ciné-micrography. Since short exposures are essential because of movement in live preparations and reciprocity failure in other cases, it is best to develop films in modern high-speed developers that do not produce an objectionable increase in photographic graininess. We use Acufine or Diafine (Baumann Photo-chemical Corp., 125 W. Hubbard St., Chicago, Illinois, USA), which provide a sensitivity gain of up to 800% above the rated film speed. All of the black-and-white photomicrographs illustrating this paper were taken on Adox KB-14 film, exposed at a rating of 21 DIN (80 ASA, setting VI/2 on the automatic exposure device of the Photomicroscope I), and developed in Acufine or Diafine.

Acknowledgments

We are grateful to Dr. H. PILLER of Carl Zeiss, for making available to us the prototype of the Zeiss/Nomarski differential equipment. Dr. C. D. WATTERS and Mr. L. F. HIRSH, JR., collaborated in various phases of the evaluation of the instrument. We are also grateful to Drs. A. BAJER (Oregon), J. GILBERT (Dartmouth), F. MUCKENTHALER (Albany), and S. M. MCGEE-RUSSELL (Albany) for preparing some of the objects illustrated in this paper Part of the work described here was carried out in the Department of Biology, Princeton University with the support of Research Grant GM-08691 from the National Institute of General Medical Science, and part at the Department of Biophysics, Columbia University Electronics Research Laboratories, New York City. The work was completed at the State University of New York at Albany under Research Grant GM-14891 from the same Institute.

Summary

The function of the differential interference microscope is explained, and the potential user is advised regarding the practical attainment of high quality images and on their interpretation. Particular attention is devoted to how the "shadow-cast" image is formed, revealing gradients of phase difference in the object. The control of contrast, the limits of resolution and detectability, optical sectioning and ways of selectively emphasizing phase and amplitude objects are discussed. A number of practical examples are presented by means of photographs.

Zusammenfassung

Die Funktion des Differential-Interferenz-Mikroskops wird erklärt und der mögliche Benutzer in bezug auf die praktische Erzielung einer hohen Qualität der Bilder und deren Interpretation beraten. Besondere Aufmerksamkeit ist hierbei der Frage gewidmet, wie das „shadow-cast"-Bild, das die Phasendifferenz-Gradienten sichtbar macht, zustande kommt. Des weiteren werden die Steuerung des Kontrastes, die Grenzen der Auflösung und Erkennbarkeit, optische Schnitte und Wege zur selektiven Hervorhebung von Phasen- und Amplitudenobjekten diskutiert. An Hand von Fotografien wird eine Anzahl praktischer Beispiele gezeigt.

Résumé

L'article décrit le fonctionnement du microscope à interférences différentielles et conseille l'utilisateur pour l'obtention pratique d'images de haute qualité et pour leur interprétation.

Les auteurs ont attaché une importance particulière à la formation de l'image „shadow-cast" qui fait apparaitre les gradiants des différences de phase.

Sont discutés en outre le règlage du contraste, les limites de résolution et de discrimination, les sections optiques et la mise en évidence sélective des objets de phase et des objets d'amplitude. Un certain nombre de photographies présentent une série d'exemples pratiques.

References

Nomarski, G.: Brevet français No. 1,059,123 (1952) [see also US Patent No. 2,924,142, granted in 1960].

— J. Phys. Radium *16*, 9 (1955).

— and A. R. Weill: Rev. de Métallurgie *52*, 121 (1955).

Piller, H.: Zeiss Mitteil. *2*, 309 (1962).

Zeiss phase contrast and interference contrast. Zeiss-Publication 41-210-e (1968) [see also Zeiss Informationen No. 70 (15. 10. 68) p. 14, and No. 71 (15. 1. 69) p. 12].

Allen, R. D., G. B. David and L. F. Hirsh, Jr.: Proc. R. micr. Soc. *1*, 141 (1966).

David, G. B., R. D. Allen, L. F. Hirsh, Jr., and C. D. Watters: Proc. R. micr. Soc. *1*, 142 (1966).

Bajer, A., and R. D. Allen: Science, N. Y. *151*, 572 (1966 a).

— — J. Cell Sci. *1*, 455 (1966 b).

Françon, M.: Mikroskopie *8*, 260 (1953).

— Progress in microscopy. London, Pergamon Press (1961).

— and T. Yamamoto: Optica Acta *9*, 395 (1962).

Swann, M. M., and J. M. Mitchison: J. exp. Biol. *27*, 226 (1950).

Inoué, S.: Exp. Cell Res. *3*, 199 (1952).

David, G. B.: Cytoplasmatic networks in neurons — a study in comparative biophysics. „Comparative Neurochemistry" — Proceedings of the 5th International Neurochemical Symposium, Austria, 10.—15. June 1962. Oxford-London-New York-Paris 1964

Barer, R.: Nature Lond. *169*, 366 (1952).

Davies, H. G., and M. H. F. Wilkins: Nature Lond. *169*, 541 (1952).

Ross, K. F. A.: Phase contrast and interference microscopy for cell biologists. London, Arnold (1967).

Gahm, J.: Die Interferenzfarbtafel nach Michel-Lévy. Zeiss-Werkzeitschrift *10* (Heft 46), 118—127 (1962).

ABBE, E.: Die Lehre von der Bildentstehung im Mikroskop von E. ABBE (edited by O. LUMMER and F. REICHE, JR.). Braunschweig, Vieweg (1910).
KOESTER, C. J., H. OSTERBERG and H. E. WILLMAN: J. Opt. Soc. Amer. *50*, 477 (1960).

[Eingegangen am 2. Dez. 1968]

Anschrift der Verfasser:
R. D. Allen, Department of Biological Sciences, State University of New York, Albany, N. Y. 12203/USA.
G. B. David, Department of Biological Sciences, University of Denver, Denver, Colorado 80210/USA.
G. Nomarski, Institut d'Optique, Centre National de la Recherche Scientifique, Paris/France.

S 41-210,6-e Printed in West Germany III/70 Boo